Modeling of snRNP Motion in the Nucleoplasm

Michaela Blažíková[1], Jan Malínský[*,2] , David Staněk[3] and Petr Heřman[1]
[1]Charles University Prague, Faculty of Mathematics and Physics, Prague, Czech Republic,
[2]Institute of Experimental Medicine ASCR, v.v.i., Vídeňská 1083, 142 20 Prague 4, Czech Republic,
[3]Institute of Molecular Genetics ASCR, v.v.i., Vídeňská 1083,142 20 Prague 4, Czech Republic
*Corresponding author: malinsky@biomed.cas.cz

Abstract: Small nuclear ribonucleoprotein particles (snRNPs) are essential supramolecular complexes involved in pre-mRNA splicing, the process of post-transcriptional RNA modifications. The particles undergo complex assembly steps inside the cell nucleus in a highly dynamic compartment called the Cajal body. We have previously shown that the free diffusion model does not fully describe the snRNP motion when tested for 1D fundamental solution of the diffusion equation. Numerical solutions of the diffusion equation were used instead to fit the experimental data obtained by fluorescence microscopy of a single cell in order to test the influence of geometry, dimensionality and boundary conditions. Finally, optimal characteristics of the model were determined.

Keywords: snRNP, diffusion

1. Introduction

Cajal bodies (CBs) are nuclear domains found in metabolically active cells [1,2]. Somatic cells contain usually 2-4 round-shaped CBs 0.5-1 μm in diameter [3]. The molecular factors found in CBs are involved in the pre-mRNA splicing, the histone pre-mRNA maturation, and in the pre-rRNA processing [4,5,6].

The pre-mRNA splicing is a two-step reaction catalyzed by spliceosomes. Spliceosomes are large complexes of hundreds of proteins containing small nuclear ribonucleoprotein particles (snRNPs), namely U1, U2, U4, U5 and U6 [7]. All spliceosomal snRNPs except the U6 contain Sm proteins that make up an extremely stable Sm core of the snRNP, while the U6 snRNP interacts with similar Like-Sm (LSm) proteins [6]. Both the Sm and the LSm proteins assemble into snRNPs during maturation and remain stably associated there.

Cajal bodies were shown to be sites of the snRNPs assembly [8,9,10]. The snRNPs form an active spliceosome that enables the pre-mRNA splicing to proceed. Spliceosomes are then inactivated and disassemble for further rounds of splicing. It has been recently shown that the snRNPs reassemble in CBs after splicing [11].

Currently no model that would describe dynamics of the snRNPs in vivo is available. A lack of metabolic energy necessary for an active movement of intra-nuclear proteins and RNA was reported in many studies [e.g. 12]. This strongly suggests that these molecules and complexes undergo a passive diffusive movement in the nucleus.

Considering this knowledge, we have previously tested whether the simplest model based on a free diffusion of snRNPs could describe movement of the particles in the nucleus [13]. An extended set of diffusion data describing spreading of the photoactivated protein complex was acquired at different locations in the nucleoplasm of 50 HeLa cell nuclei. A global fitting of the data to the fundamental solution of the diffusion equation in 1D indicated that the spreading of the complex has a diffusion character. However, the free diffusion model with a global and spatially invariant diffusion coefficient D was inconsistent with the data and could not explain the dynamics of the snRNP particles in the nucleoplasm. Individual analysis of the diffusion curves revealed that the D value increases with increasing radial distance from the photoactivated CB. In the first approximation $D(x)$ depends linearly on the distance x, $D(x) = D_0 + \Delta D \cdot x$, where D_0 = $(4.7\pm5.4)\times10^{-14}$ m^2/s and ΔD = $(3.7\pm0.6)\times10^{-8}$ m/s [13].

In order to eliminate a possible variability of environment in different cell nuclei, in this study we performed similar measurements and analyses on a single nucleus. We also examined influence of dimensionality of the solved problem on the obtained results. D was therefore

evaluated using 1-, 2- and 3-dimensional model of the nucleus. Finally, accuracy and applicability of the models was tested and discussed.

2. Methods

2.1 Live cell imaging

HeLa cells were co-transfected with two fluorescently labeled proteins. The first one was SART3 tagged with the cyan fluorescent protein (SART3:CFP). SART3 is known to accumulate in Cajal bodies and was therefore used as a CBs marker to visualize and localize them in the nucleus. The second protein was SmB, one of the Sm proteins taking part in the snRNP complex formation. This protein carried a photoactivatable green fluorescent protein tag (PA-GFP) that can be converted from non-fluorescent to fluorescent form by ~400 nm laser light illumination [14]. It has been recently reported that SmB:PA-GFP proteins remain stably associated with the snRNP complex after its formation [11]. Spreading and distribution of the complex can be therefore followed by fluorescence after the local photoactivation of SmB:PA-GFP. The cells were imaged by the Zeiss LSM 510 confocal microscope equipped with a 63x/1.2 NA water immersion objective. Three images were acquired before the photoactivation. Then the SmB:PA-GFP localized in one selected CB was photoactivated by a short laser pulse at 405 nm and time series of fluorescence images was acquired for 5 minutes with 15s increments for each of the selected nuclei. For the fluorescence imaging the SmB:PA-GFP and SART3:CFP complexes were excited at 488 nm and 458 nm, respectively, and their emission was collected into two channels through the long-pass LP505 and the band-pass BP470-500 filters, respectively.

2.2 Image processing

Images were analyzed using the Matlab software. Images from the cyan channel (SART3:CFP) were used to identify locations of Cajal bodies before the photoactivation. Fluorescence intensity of the photoactivated complexes (SmB:PA-GFP) was evaluated from the green channel images. After the photoactivation, tracking by means of the thresholding was used to identify and follow a slight motion of the photoactivated CB. Time course of the fluorescence intensity of SmB:PA-GFP was evaluated in the nucleoplasm at properly chosen distances from the photoactivated CB.

3. Numerical Model

3.1 Analytical fitting

The method of analytical fitting was reported in detail in [13]. Briefly, the motion of snRNPs was described by a diffusion equation with a spatially invariant diffusion coefficient *D*:

$$\frac{\partial c(x,t)}{\partial t} - D\frac{\partial^2 c(x,t)}{\partial x^2} = f\,, \qquad (1)$$

where *x* is a space coordinate, *t* denotes time, and *c* is a concentration of diffusing particles. The source term *f* was set to zero. We used an initial condition $c(x,0) = \delta(x - x_{CB})$ to simulate the photoactivation at x_{CB}, i.e. in the location of the selected Cajal body. The fundamental solution *F* of Eq.(1) can be written as [15]:

$$F(x - x_{CB}, t) = \frac{k}{2\sqrt{\pi D t}} e^{-\frac{(x - x_{CB})^2}{4Dt}}\,, \qquad (2)$$

where *k* is a multiplicative parameter describing fluorescence brightness of SmB:PA-GFP in the cell. Eq. (2) was used for a non-linear least squares (NLS) fitting [16] of the experimental data. The fitting was performed in the Matlab software (function *nlinfit*). As a result we obtained optimized parameters *D* and *k* for each dataset.

3.2 Numerical fitting

Solutions from the Diffusion Application Module (Comsol, Eq.1) were transferred to the Matlab and used for the NLS fitting of the measured intensity evolutions. In order to evaluate influence of dimensionality on the fitting results, we performed the analysis sequentially in 1D, 2D and 3D. Specific geometry was added into the model. In particular, initial conditions $c(\vec{x},0) = c_0$ for

$\vec{x} = CB$ and $c(\vec{x},0) = 0$ elsewhere simulated the photoactivation in the CB area only. Neumann boundary conditions $\vec{n}.\vec{N} = 0, \vec{N} = -D\vec{\nabla}c$ were used to define impermeability of the nuclear membrane for the diffusing particles. The fitting performed in the Matlab software yielded optimized parameters *D* and c_0 as functions of distance from the photoactivation area.

4. Experimental Results

Cajal bodies serve as spliceosomal snRNP assembly sites; the concentration of the snRNPs in CBs is substantially higher than in the nucleoplasm [3]. A population of the snRNPs confined to one selected Cajal body (CB) was photoactivated by a laser pulse. Movement of the photoactivated protein fraction was followed by the time lapse imaging. Arrangement of the experiment is shown in Fig. 1.

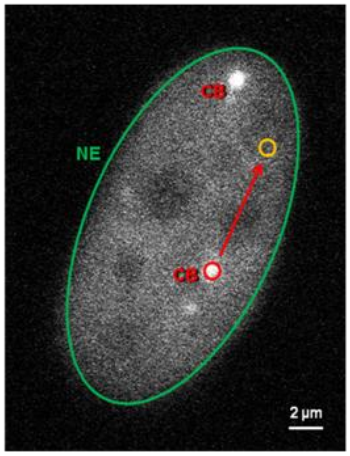

Figure 1. Arrangement of the photoactivation experiment. Diffusion of the snRNP complexes inside the nucleoplasm delimited by the nuclear envelope (NE, green) was visualized by the SmB:PA-GFP fluorescent fusion protein. PA-GFP was photoactivated within the circular area (red circle) corresponding to one of the Cajal bodies (CB). Spreading of the photoactivated complexes (red arrow) was measured in the nucleoplasmic area (yellow circle).

Diffusion coefficient was evaluated in one cell nucleus at different distances from the CB by analytical fitting of the data to the fundamental solution of the diffusion equation in 1D (see methods). For the single cell we found a similar linear dependence of *D(x)* on the radial distance *x* from the photoactivated CB (Fig.3, analytical 1D fit) as when *D* was evaluated in different cell nuclei [13]. In this case the linear regression coefficients were $D_0 = (0 \pm 1.5)\times10^{-13}$ m^2/s and $\Delta D = (7.1 \pm 0.6)\times10^{-8}$ m/s. The dependence of *D* on the distance from the photoactivated CB was tested on other 10 cell nuclei with similar results (data not shown).

In order to make modeling more realistic we applied a numerical solution of the diffusion model. On the contrary of the analytical solution, the numerical approach allows to include specific cell geometry and to add initial and boundary conditions to the model (see Methods). Geometries of the 1D and 2D models best corresponding to the real cell shape measured from Fig. 1 are schematically depicted in Fig. 2.

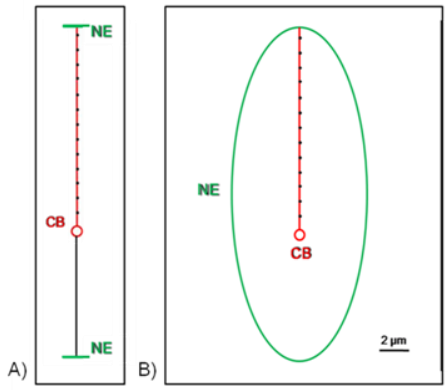

Figure 2. Model used for numerical 1D and 2D fitting. **A)** In 1D the cell nucleus was represented by a line segment of 21 µm length. Center of the CB (a line segment of 0.5 µm length) was located inside the nucleus, 8.2 µm from the lower NE end. The measurement points were located along the red line with 0.96 µm distance from each other. **B)** In the 2D model, the nucleus was represented by the ellipse (semi-axes of 10.5 µm and 5 µm) and the CB was modeled as a circle (with 0.25 µm radius) located on its major axis at 8.2 µm distance from the lower nuclear pole. The measurement points were located along the major axis with 0.96 µm distance from each other.

The 3D model was created from the 2D one by formation of an ellipsoid with the third semi-

axis of 2.5 µm. This dimension could not be measured and it was taken from the literature according to an average size of HeLa cells [3]. Positions of the CB and the measurement points remained the same as for the 2D model. Results of the NLS fitting for 1-, 2- and 3-dimensional models are shown in Fig. 3.

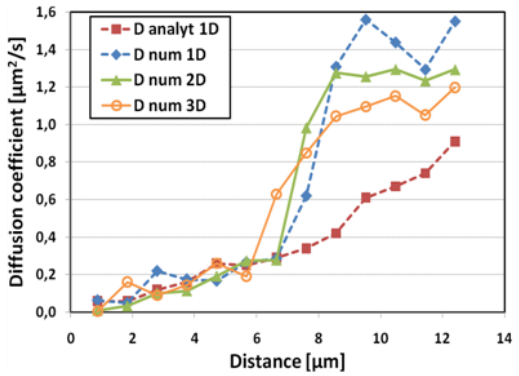

Figure 3. Evaluation of the diffusion coefficient in different distances from the photoactivated CB. Comparison of analytical fit in 1D with numerical fits in 1D, 2D and 3D.

For all the numerical models the results are qualitatively similar. As expected, for longer diffusion distances they all differ from the analytical 1D fit: instead of the continuous growth, the numerical solutions exhibit a sigmoidal shape of the *D(x)* curve with an inflection point at approx. 7 µm. This is a consequence of the added geometry and boundary conditions to the model. Fits of an example data are shown in Fig.4.

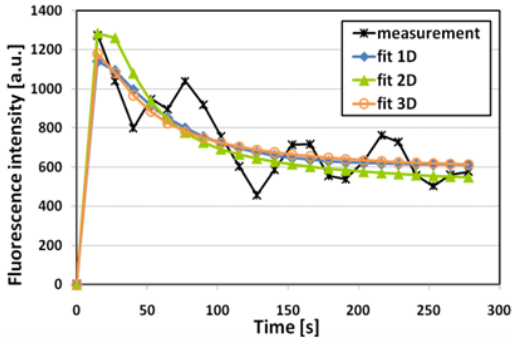

Figure 4. Example of experimental data measured in the distance of 2.8 µm from the photoactivated Cajal body (open circles) and numerical fits in 1D, 2D and 3D.

From our simulations we can conclude that the model dimensionality does not significantly affect qualitative results obtained on the improved numerical model with the specific geometry and boundary conditions. Because the 1D model does not allow to properly describe and change the cell footprint, we decided to use the 2D model for further qualitative evaluation of model properties.

In order to evaluate how accurately can be an irregular shape of the cell nucleus represented by the chosen ellipsoid, we tested a sensitivity of the recovered diffusion coefficients to changes in the model geometry, Fig. 5A. In particular, the minor axis of the ellipsoid was both elongated (I) and shortened (II). The major axis was elongated (III). Finally, we kept the original nuclear size unchanged and the CB position was moved closer to the nuclear membrane (IV). Results are summarized in Fig. 5. The elongation of the minor-axis induced a shift of the sigmoidal *D(x)* curve transition to a longer distance while shortening caused an opposite effect, Fig. 5B. The plateau of the curves remained in both cases unchanged. Diffusion coefficients at short distances were found to be slightly lower and higher for shorter and longer minor-axis, respectively. The elongation of the major-axis induced slower growth of *D(x)* and a dramatic shift of the transition point to even longer distances, Fig. 5C. The plateau of *D(x)* was not reached and it was probably shifted out of the analyzed area.

The relocation of the CB with the linked measurement positions closer to the nuclear envelope caused a slight increase of the diffusion coefficient at short distances (similar to the case II). Moreover, a slower growth of the curve and a plateau elevation, similar to the case III, was observed, Fig. 5C. These results reveal a strong dependency of the calculated diffusion coefficient on the position of the CB within the nucleus.

In summary, model geometry as well as positions of the measurement points in the nucleoplasm was found to have a considerable effect on the fitted values of the apparent diffusion coefficient. For quantitative evaluation of D within a cell nucleus it is therefore imperative to use a detailed shape of the particular nucleus and to accurately model position of the photoactivated Cajal body within the nucleus.

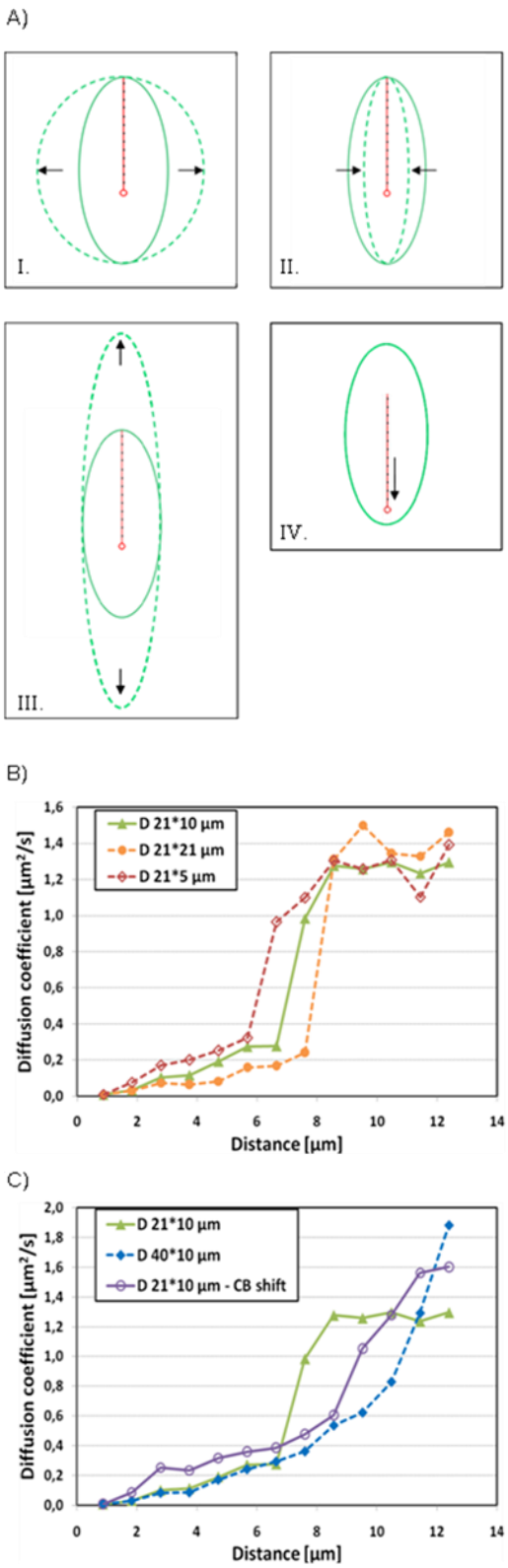

Figure 5. Effect of geometry changes on the apparent diffusion coefficient in the 2D model. **A)** Scheme of the geometry changes. Elongation of the minor axis from 10 µm to 21 µm (I) and shortening the axis from 10 µm to 5 µm (II). Elongation of the major axis from 21 µm to 40 µm (III) and change of the CB position within the nucleus (IV). The red line indicates the analysis area. **B)** Effect of the minor axis change (configurations I and II). **C)** Effect of the major axis elongation (III) and the CB position change (IV).

5. Discussion

Consistently with previous results obtained on a set of cells [*Blazikova et al.*, 2008] the current diffusion analysis restricted to data from a single cell nucleus indicate that the value of the apparent diffusion coefficient increases with increasing radial distance from the photoactivated Cajal body. This qualitative observation was found to be independent of major model-geometry changes. Mechanisms underlying the observed spatial dependence of the diffusion coefficient remain unknown at present. We propose that the effect could result from interactions of the diffusing particles with other large macromolecular complexes in the nucleus. Such interactions should modulate the value of the apparent diffusion coefficient obtained at different locations in the nucleus. Construction of a model that includes such interactions is in progress.

6. Conclusions

Our study of the snRNP dynamics within the single cell nucleus shows that the snRNP motion cannot be explained in the terms of free diffusion. The apparent diffusion coefficient of SmB:PA-GFP was found to show a significant dependence on the distance from the photoactivated Cajal body. Essentially the same result was obtained for 1D, 2D and 3D models. Dependency of the apparent diffusion coefficient on the model geometry revealed that a detailed knowledge of the nuclear shape is crucial for the accurate modeling. Our calculations indicate that data from different cell nuclei cannot be analyzed together by a common model based on an "average" nucleus geometry. Instead, each

nucleus has to be modeled and analyzed separately.

7. References

1. Boudonck, K., et al., Coiled body numbers in the Arabidopsis root epidermis are regulated by cell type, developmental stage and cell cycle parameters, *Journal of Cell Science*, **111**, 3687-3694 (1998)
2. Pena, E., et al., Neuronal body size correlates with the number of nucleoli and Cajal bodies, and with the organization of the splicing machinery in rat trigeminal ganglion neurons, *The Journal of Comparative Neurology*, **430**, 250-263 (2001)
3. Klingauf, M., et al., Enhancement of U4/U6 Small Nuclear Ribonucleoprotein Particle Association in Cajal Bodies predicted by Mathematical Modeling, *Molecular Biology of the Cell*, **17**, 4972-4981 (2006)
4. Gall, J. G., Cajal bodies: the first 100 years, *Annual Review of Cell and Developmental Biology*, **16**, 273-300 (2000)
5. Matera, A. G. and K. B. Shpargel, Pumping RNA: nuclear bodybuilding along the RNP pipeline, *Current opinion in cell biology*, **18**, 317-324 (2006)
6. Stanek, D. and Neugebauer K. M., The Cajal body: a meeting place for spliceosomal snRNPs in the nuclear maze, *Chromosoma*, **115**, 343-354 (2006)
7. Jurica, M. S. and M. J. Moore, Pre m-RNA splicing: awash in sea of proteins, *Molecular Cell*, **12**, 5-14 (2003)
8. Schaffert, N., et al., RNAi knockdown of hPrp31 leads to an accumulation of U4/U6 di-snRNPs in Cajal bodies, *EMBO Journal*, **23**, 3000-3009 (2004)
9. Stanek, D. and Neugebauer K. M., Detection of snRNP assembly intermediates in Cajal bodies by fluorescence resonance energy transfer, *The Journal of Cell Biology*, **166**, 1015-1025 (2004)
10. Nesic, D., et al., A role for Cajal bodies in the final steps of U2 snRNP biogenesis, *Journal of Cell Science*, **117**, 4423-4433 (2004)
11. Stanek, D., et al., Spliceosomal snRNPs Repeatedly Cycle through Cajal Bodies, *Molecular Biology of the Cell*, **19(6)**, 2534-2543 (2008)
12. Dundr, M., et al., In vivo kinetics of Cajal body components, *The Journal of Cell Biology*, **164**, 831-842 (2004)
13. Blazikova M., et al., Diffusion Modeling of snRNP Dynamics, *WDS'08 Proceedings of Contributed Papers: Part III - Physics*, in press (2008)
14. Patterson, G. H. and J. Lippincott-Schwarz, A Photoactivable GFP for Selective Photobleaching of Proteins and Cells, *Science*, **297**, 1873-1877 (2002)
15. Itô S., *Diffusion equations*, 25-39. American Mathematical Society (1992)
16. Johnson, M. L., Use of Least-Squares Techniques in Biochemistry, *Methods in Enzymology*, **240**, 1-36 (1994)

8. Acknowledgements

This work was supported by the Grant Agency of the Czech Republic (204/07/0133), by the Grant Agency of Charles University (79508, to M.B.) and by the Ministry of Education, Youth and Sports of the Czech Republic (MSM 0021620835, to P.H.).